The Interpretation of Forces Involving Deformable Interfaces

Sarah A. Nespolo[1], Patrick G. Hartley[2], Michael A. Bevan[1], Derek Y. C. Chan[3], Franz Grieser[4], and Geoffrey W. Stevens[1]

[1]Department of Chemical Engineering
[3]Department of Mathematics and Statistics
[4]School of Chemistry
The University of Melbourne, Parkville, VIC, 3010, Australia.

[2]CSIRO Molecular Science
Clayton South, VIC, 3169, Australia.

Quantitative understanding of the forces acting at liquid-liquid interfaces and how they are influenced by various additives is important in many chemical engineering applications. For example, the control of emulsion stability is a major concern in many commercial products and industrial processes.

The measurement of interfacial forces between two surfaces as a function of separation provides direct information on the relationship between effects of specific additives and system stability. The interaction forces between a silica colloidal particle and an immobilized hydrocarbon droplet in an aqueous medium have been measured using the Atomic Force Microscope. Force-distance relationships for an anionic surfactant have been measured over a range of concentrations.

A theoretical model that calculates the force between a rigid spherical probe particle (attached to an AFM cantilever) and a liquid interface has been examined. A key parameter in this model, the electrostatic surface potential, was inferred from measurement of electrophoretic mobilities of dispersed oil droplets. The interpretation of an oil droplet's surface potential from its mobility in an electric filed is the same as for a hard particle, except that the effect of interfacial momentum transfer on the droplet drag coefficient must be considered. Although the theoretical solution for a fluid droplet's drag coefficient is well known, its experimental measurement is difficult and its interpretation is complicated due to adsorbed surfactant and the possibility of droplet deformation. Interpretation of experimental electrophoretic mobilities requires independent measurements of particle size, shape, and amount of adsorbed surfactant.

INTRODUCTION

The measurement of surface forces has, for many years, been the focus of much interest in the field of colloid and surface science.[1] This is principally due to the fact that the long-range interactions between particles controls the ability of a dispersion to resist coagulation/flocculation. In addition, the rheology of dispersions is determined to a large degree by inter-particle forces. The interaction of solid colloidal particles with deformable liquid interfaces is of fundamental interest in many technologically important areas such as mineral processing, fluid-fluid processing, and biomedical technologies. An understanding of the surface forces acting between solid-water and oil-water interfaces is a critical factor in the control of the adhesion and transfer of particulate material in aqueous and nonaqueous media.

The measurement of surface force interactions involving liquid particles is complex due to interfacial fluidity and deformability. It is known that these two features have a great impact on the hydrodynamic interactions and the resulting dynamic properties of such systems[2-7]. They are particularly important for the kinetic stability of emulsions against coalescence[2-4]. Interactions involving deformable interfaces are typically interpreted using measurements of single properties, such as contact angle, interfacial tension, and electrophoretic mobility. Such measurements alone provide a qualitative correlation with long range interactions in such systems, but are unable to describe the response of a deformable interface to the force field of an approaching particle or surface[8]. In this study, the development of an experimental technique to measure the forces involved in the interaction of deformable surfaces is shown. Although, the AFM has routinely been used to measure force-separation profiles for the interaction of solid surfaces, only recently have measurements involving deformable surfaces appeared in the literature. The difficulty with measurements involving a deformable surface is the lack of an interpretive theoretical model.

In the present study, we make independent measurements of droplet surface potential, so that in conjunction with the interpretive theory[9], it is possible to quantitatively understand the measured forces operating at liquid-liquid interfaces. The measurement of the droplet surface potential has inherent complexities due to the possibility of momentum transfer across the liquid-liquid interface. Thus an understanding of the droplet hydrodynamics is essential for converting the electrophoretic mobility, μ, to ζ-

potential[10, 11]. In this study we have employed, both static and dynamic light scattering to provide direct information concerning the droplet hydrodynamic mobility coefficient, α. Static light scattering (SLS) is used to measure droplet shape and size, and dynamic light scattering (DLS) is used to measure droplet diffusion from which the hydrodynamic mobility coefficient is determined. With measurement of these independent parameters, the effect of internal droplet flow on the droplet hydrodynamic mobility coefficient can be determined unequivocally. Additional measurements of interfacial tension are then used to compare the ζ-potential, droplet surface charge, and the amount of adsorbed surfactant. These data allow the correct ζ-potentials to be chosen which correspond to reasonable values of the degree of ionization, or the degree of counter-ion binding, of sodium ions with surfactant molecules at the droplet surface.

EXPERIMENTAL SECTION

A Digital Instruments (Santa Barbara, CA) Nanoscope IIIa AFM was used to measure forces between colloidal silica and an *n*-decane, oil droplet as shown in Fig. 1. Experimental details are described in detail elsewhere[12].

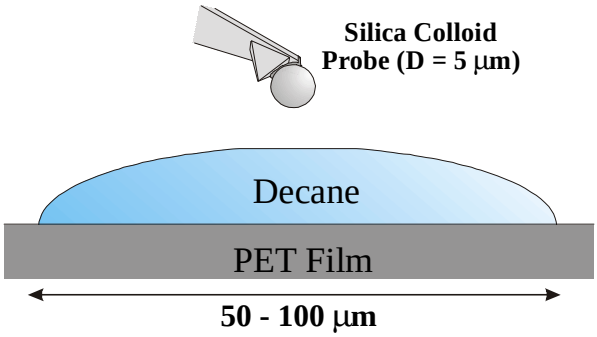

Figure 1: Schematic of the AFM experiment between a Silica Colloidal Probe (R≈2.5μm) and an Immobilized Decane Droplet.

The aqueous SDS/decane emulsions were prepared by rapidly injecting decane into a background solution of 0.1 M SDS and 1 mM $NaNO_3$ to give a droplet volume fraction of ~10^{-5}. This mixture was shaken and then sonicated for 1 hour. The desired background SDS concentration was obtained by further dilution with 1 mM $NaNO_3$ followed by additional shaking and sonication. These solutions were allowed to stand overnight prior to light scattering or electrophoresis measurements the next day.

With 10 measurements per sample, electrophoretic mobilities were made using a Coulter DELSA 440 laser Doppler apparatus. Control studies of SDS/decane electrophoretic mobilities at 2.00, 5.00, 10.0, and 20.0 V/cm indicated a linear response with electric field strength. Reported data was obtained at 5.00 V.

Droplet samples were prepared at low volume fractions suitable for light scattering experiments so that further dilution was not required. Static Light Scattering measurements were performed at twenty angles between 30 and 140 degrees with typical measurement times of 100 seconds at each angle. Dynamic Light Scattering measurements were each performed at several angles using delay times and total scan times optimized with the aid of instrument software. Interfacial tension data were obtained from static measurements using a commercial pendant droplet instrument.

RESULTS AND DISCUSSION

Forces between a Rigid Probe Particle and a Liquid Interface

The disjoining pressure between a rigid spherical probe particle attached to an AFM cantilever and a liquid interface is treated in an analytic manner to describe the total force exerted on the probe as a function of the distance of the probe from the rigid substrate, the AFM stage, on which the liquid interface resides[9]. For a given disjoining pressure, $\Pi(D)$, the theory calculates the total force on the interface and the separation. The disjoining pressure is calculated from the numerical solution of the full Poisson-Boltzmann equation between flats for 1:1 electrolyte with constant charge boundary conditions, solving using the method of Chan *et al.*[13]. The planar Poisson-Boltzmann equation is

$$\frac{d^2Y}{d\xi^2} = \sinh Y \,, \qquad (1)$$

where *Y* is the scaled potential, $Y = \frac{e\psi}{kT}$, and ξ (κx) is the scaled distance measured from the midplane.

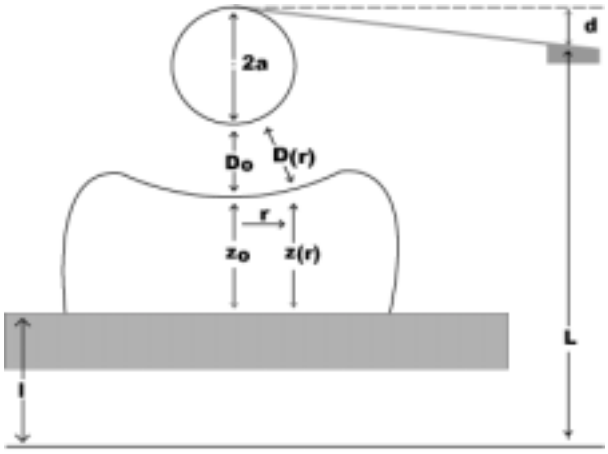

Figure 2: Geometry of AFM measurement detailing the relevant parameters required for the theoretical model. *L* is fixed and hence constant, *d* is the cantilever deflection measured using the photodiode, *l* is the stage displacement, 2a is the diameter of the probe, z_o is the central distance of the droplet and D_o is the central distance between the droplet and the probe. (The deformation is not shown to scale)

$$F = K_c d \tag{2}$$

where *F* is the force and K_c is the spring constant of the AFM cantilever and from geometry,

$$\frac{F}{K_c} = z_o + D_o + l + \text{constants} \tag{3}$$

where *F* is the force and K_c is the spring constant of the AFM cantilever.

For a solid system, z_o is constant, and the force can be determined since D_o is constant at large forces (constant compliance region). For a purely elastic system, K_d is the effective spring constant of the interface and $z_o = \frac{F}{K_d}$, and again this equation can be solved. Since the system here is neither solid nor elastic, the Young-Laplace equation is modified and an equation for z_o is obtained.

The profile of the inner part of the droplet can be described by the following differential equation,

$$D'' + \frac{1}{t}D' - \left(2\left(1 + \frac{a}{R_o}\right) - \frac{a\Pi(D)}{\gamma}\right)D_o = 0 \tag{4}$$

where $t = \frac{r}{\sqrt{D_o a}}$, *r* is the radial length, R_o is the radius of the oil droplet and γ is the interfacial tension.

The total force on the interface (in the Derjaguin approximation) is

$$F(D_o) = 2\pi\gamma G(D_o) \tag{5}$$

Matching the outer solution of the inner profile and the inner solution of the outer profile of the droplet, results in a relationship for z_o and *F* in terms of D_o.

$$X = z_o + D_o = H + G\left[P(\theta_c) + \log\frac{\sqrt{D_o a}}{2R_o}\right] + \text{constants} \tag{6}$$

where *G* and *H* are expressions involving the disjoining pressure,

$$G = \frac{aD_o}{\gamma}\int_o^t dtt\Pi(D(t))$$

$$H = \frac{aD_o}{\gamma}\int_o^t dtt\ln t\Pi(D(t))$$

and $P(\theta_c)$ is a function of contact angle, θ_c. Since z_o and D_o are not separable, *X* is defined as the vertical distance between the origin fixed to the stage and the lowest point on the probe sphere, $X = z_o + D_o$

From Equs. (5) and (6), F^{theory} and $X(D_o)$ are obtained. Details can be found in Chan *et al.*[9]. Δl_{theory} can then be determined from Equ. (2)

$$(\Delta l)_{theory} = (\Delta d)_{theory} - (\Delta X(D_o))_{theory} + \text{constants} \quad (7)$$

The mathematical model is used to determine the absolute separation between the deformable interface by comparing $\frac{F_{theory}}{a} vs\, \Delta l_{theory}$ with $\frac{F}{a} vs\, \Delta l$ obtained from AFM measurements. It is clearly shown in Equs. (1) and (4) that the experimental parameters; surface potentials at infinite separation, ψ, interfacial tension, γ, Debye length, κ^{-1}, and probe radius, a, are integral in the solution of the droplet profile and hence, the interpretation of the theory. To fully interpret the surface force measurements presented in the following section, knowledge of the true separation between the solid-liquid interface is required. This is a critical ingredient for developing an understanding of the apparent interplay between interfacial deformation and double layer interactions observed in these experiments and has important implications in understanding both emulsion stability and wetting phenomena.

Forces between a silica colloidal probe and an *n*-decane interface measured by AFM.

The interaction forces for a negatively charged silica colloidal probe approaching an *n*-decane interface in varying concentrations (10^{-4} M to 10^{-2} M) of a 1:1 electrolyte have been measured. At large separations, it was found that there is excellent agreement with DLVO theory, but as the relative separation distance of the colloidal probe and the oil interface is decreased, deviations are observed. This results in a second interaction regime, with the interactions changing from an exponential to a simple linear relationship at larger forces. Instantaneous engulfment (at which point deflection data became immeasurable) of the silica colloidal probe by the *n*-decane droplet eventually occurs at one point in the force-separation profile. Results obtained demonstrate that non polar surfaces prepared in this way acquire a significantly negative diffuse layer potential in electrolyte solutions, as indicated by force distance relationships which obey DLVO theory at large separations. It has been hypothesised[12], that the observed deviation from experimental behaviour at high forces may be due to the interface deforming and "wrapping" around the particle with the interface thus being driven away as the particle is pushed toward it.

In Fig. 3, the effect of the introduction of various concentrations of SDS, on the interaction forces between a silica colloidal probe and the *n*-decane interface in a 10^{-3} M $NaNO_3$ background electrolyte is shown. Engulfment, as found in the pure electrolyte has been completely removed by the addition of surfactant. As the concentration of surfactant was increased, there was a reduction in the slope of the pseudolinear regime for stronger forces. At these separations, a small decrease in the relative separation results in a large increase in force.

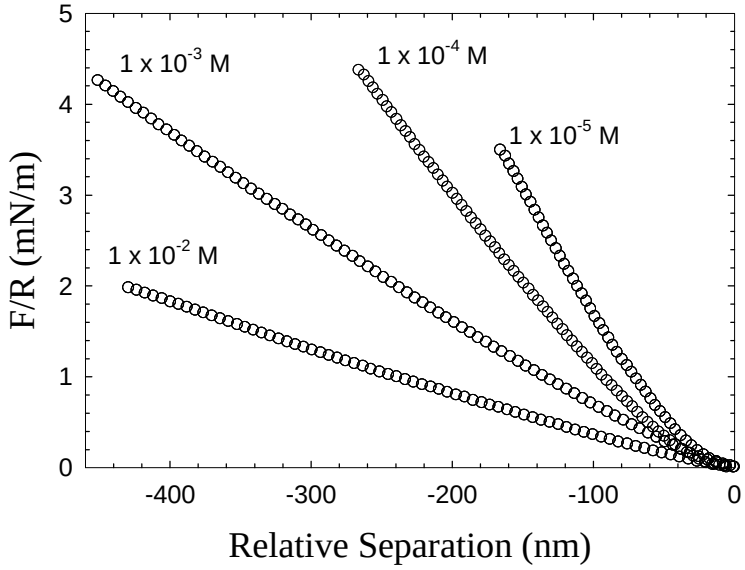

Figure 3: Measurement of surface forces between a silica colloidal probe and the *n*-decane-aqueous interface in 10^{-3} M $NaNO_3$, pH 5.6, at different concentrations of SDS. With the addition of SDS, concentrations above 10^{-5} M, the engulfment of the silica colloidal probe into the decane was eliminated.

Zero separation, for solid-solid interactions, is defined as the location where a change in the piezo voltage results in an equal change in the photodiode voltage caused by the deflection of the cantilever. This definition is not applicable for a deformable interface. In Fig. 3 a relative separation has been used by defining zero separation to be when the force divided by the radius (F/R) is equal to 0.01 mN/m. To determine the absolute separation, comparison of theory and experiment needs to be made.

A parameter of the theoretical model is the oil droplet surface potential which needs to be determined independently. The surface potential, ψ, is defined to occur at the rigid particle surface, and is not necessarily the same as the electrokinetically relevant ζ-potential, which occurs at the plane of shear next to the charged interface. For the purpose of this study, it is adequate to assume that $\psi \approx \zeta$.

Most droplet electrophoresis studies in the literature assume that the droplet behaves like a solid particle as far as its hydrodynamic properties are concerned and use the theory of Smoluchowski[14] to interpret the droplet shear surface potential, or ζ-potential. The Smoluchowski result is reasonable in the limit of thin double layers and low potential for solid particles, but for oil droplet studies it may not be valid to assume solid particle hydrodynamics without support from independent measurements[10, 11, 15-19]. Several oil droplet electrophoresis studies[20-22] have used the O'Brien and White (OW) theory[23], but have avoided the issue of droplet hydrodynamics. In order to interpret the electrophoretic mobilities of oil droplets, we use the theory of Ohshima *et al.*[16] which extends the OW model to include hydrodynamic effects.

Interpretation of ζ-potential from Electrophoretic Mobilities of Aqueous SDS/decane Droplets

A steady particle velocity, or electrophoretic mobility results when an electric field is applied to a charged particle in aqueous solution. For a charged oil droplet in water, the electrophoretic mobility, μ, determined experimentally, can be related to the ζ-potential by

$$\mu = \frac{U}{E} = -\frac{\beta(\eta_i/\eta_o, \zeta, \kappa a)}{\alpha(\eta_i/\eta_o, \zeta, \kappa a)} \tag{8}$$

where U is the velocity of a charged particle moving in the presence of a weak electric field is linearly related to the strength of the applied field, E. η_i is the viscosity of the fluid inside the droplet, η_o is the viscosity of fluid outside the droplet, ie. the continuous medium viscosity, α is the hydrodynamic mobility coefficient and β is a coefficient that must be computed from theory[16, 23].

The interpretation of measured electrophoretic mobilities, μ to ζ-potentials of immiscible oil droplets is more complex than for solid particles because of the associated droplet hydrodynamics. The hydrodynamic mobility coefficient, for a liquid droplet moving though a fluid, can be considerably less than that for a solid particle because of the ability for momentum to be transferred across the droplet's oil-water interface into the interior of the oil droplet, which produces internal flow or circulation. In Table 1 electrophoretic mobilities, μ, are listed for decane droplets in 1 mM $NaNO_3$ and varying bulk SDS concentrations which are all below the critical micelle concentration (CMC).

Table 1: Electrophoretic measurements of decane droplets in aqueous SDS solutions and 10^{-3} M $NaNO_3$ at 298K.

	1x10^{-3} M SDS	**1x10^{-4} M SDS**	**1x10^{-5} M SDS**
μ (μm/s)(V/cm)	-5.30 ± 0.27	-5.65 ± 0.20	-5.70 ± 0.20

Table 2. The magnitude of the ζ-potentials ranges (mV) from electrophoretic mobility and the normalized hydrodynamic mobility coefficient $\alpha/(\pi\eta a)$ as determined from light scattering experiments at 298K.

$\lvert\zeta\rvert$-potentials (mV)	***α/(πηa)***	**1 x 10^{-3} M SDS**	**1 x 10^{-4} M SDS**	**1 x 10^{-5} M SDS**
Liquid 1	5.1	13-14	13-14	11
Liquid 2	6.1	182-194	179-187	190-194
Solid 1	6.2	90-127	108-148	94-112
Solid 2	6.2	127-173	-	154-176

In Table 2, μ (displayed in Table 1) have been converted into ζ-potentials using standard electrokinetic theories, O'Brien and White[23] and Ohshima *et al.*[16]. Also tabulated, are the normalized hydrodynamic mobility coefficient, $\alpha/(\pi\eta a)$ for each ζ-potential. The 3 highest ζ-potentials in Table 2 all have $\alpha/(\pi\eta a) \approx 6$

even though the highest potential corresponds to the liquid droplet case. In the limit of high surface potential, internal droplet flow does not play an obvious role when interpreting μ, at least in terms of effects on α.

Depending on whether one assumes the droplet behaves hydrodynamically as a solid particle or as a liquid particle, each measured electrophoretic mobility value can allow up to 4 possible corresponding ζ-potentials, as opposed to at most 2 solutions for solid particles. It is therefore necessary to acquire additional experimental information to obtain a unique ζ-potential for each experimentally measured electrophoretic mobility.

Interpretation of ζ-potentials from Measurements of Droplet Hydrodynamics using Static and Dynamic Light Scattering

As the previous section discussed, it is essential to measure the hydrodynamics independently of the electrokinetics. The present experimental investigation reveals how the hydrodynamics of a submicron hydrocarbon droplet can be measured using static and dynamic light scattering. In order to measure the droplet hydrodynamics, independent and self-consistent measurements of the droplet's hydrodynamic mobility coefficient, shape and size are required. The hydrodynamic mobility coefficient, α, of an uncharged sphere of radius, *a*, for Stokes flow in an unbounded fluid is,

$$\alpha = 6\pi\eta_o a \tag{9}$$

The diffusion coefficient, *D*, and hydrodynamic mobility coefficient, of a single spherical particle for infinitely dilute conditions are related via the Stokes-Einstein equation,

$$D = \frac{kT}{\alpha} \tag{10}$$

where *k* is Boltzmann's constant and *T* is absolute temperature. The droplet diffusion coefficient is measured using Dynamic Light Scattering. While DLS provides a measure of the droplet α, it provides no additional information that allows α to be interpreted in terms of the physical properties of the droplet. Determining the degree of momentum transfer at the droplet surface requires independent knowledge of the droplet size and shape in order to fully understand the hydrodynamics. The more general result for the mobility coefficient of any spherical droplet with a continuity of shear stress hydrodynamic boundary condition at the droplet surface is[24],

$$\alpha(\lambda) = f(\lambda)6\pi\eta_o a \tag{11}$$

where, $f(\lambda) = \dfrac{2/3 + \lambda}{1 + \lambda}$ and $\lambda = \dfrac{\eta_i}{\eta_o}$ (12)

The two limits for the hydrodynamic mobility coefficient is (1) for an infinite droplet viscosity ($\lambda \to \infty$), which reduces to a solid particle, $\alpha(\lambda) = 6\pi\eta_o a$ and (2) for an inviscid fluid droplet ($\lambda \to 0$), such as an air bubble, $\alpha(\lambda) = 4\pi\eta_o a$. For the liquid system dealt with here, the hydrodynamic mobility coefficient is

$$\alpha\left(\frac{\eta_{Decane}}{\eta_o}\right) = 5.02\pi\eta_o a \tag{13}$$

In addition to the effects of internal flow, the oil droplet hydrodynamic mobility coefficient, α, is further complicated by an additional dissipative mechanism due to droplet surface charge, which is essentially the "primary electroviscous effect"[10]. For a charged particle moving through a fluid, ions associated with the electrical double layer distort the local flow field of the surrounding fluid. Fluid flow near any charged particle surface experiences an "electroviscous" drag because of the tendency for the associated spatial ion distribution near the surface, or electrical double layer, to resist distortion in the flow field. For the solid particle model with $\alpha/(\pi\eta a)$=6 for ζ=0, $\alpha/(\pi\eta a)$ rises gradually to ~6.02 in the limit of high potential. For the liquid droplet model, $\alpha/(\pi\eta a)$ initially starts at the decane/water limit around $\alpha/(\pi\eta a)$=5 for ζ=0, and then increases to ~6.02 in the limit of high potential. This indicates that "electroviscous" effects dominate the hydrodynamic mobility coefficient in the high ζ-potential limit and completely mask any effects due to internal droplet flow. As a result of the dominant "electroviscous" contribution for the droplets in the limit of high potential, the liquid droplet and the solid particle solutions have the same value of α for high potentials. As a result, the potential at the plane of shear on the droplet surface, or the ζ-potential, and the

scaled thickness of the double layer, κa, are important in determining additional dissipative effects embodied in Equ. (11) as,

$$\alpha(\lambda,\zeta,\kappa a) = f(\lambda,\zeta,\kappa a)6\pi\eta_o a \tag{14}$$

where $f(\lambda,\zeta,\kappa a)$ can be evaluated using electrokinetic theory,[23] and κ is the inverse of the Debye length.

It is possible to determine experimentally the collective terms, $6f(\lambda,\zeta,\kappa a)$, by combining Equs. (10) and (14) and using the SLS measured droplet radius, a_{sls}, and the DLS measured diffusion coefficient, D_{dls}, to give,

$$6f(\lambda,\zeta,\kappa a) = \frac{\alpha(\lambda,\zeta,\kappa a)}{\pi\eta_o a_{sls}} = \frac{kT}{\pi\eta_o a_{sls} D_{dls}} \tag{15}$$

where the middle part of the Equ. (15) is a re-arrangement of Equ. (14) and the right hand side is a re-arrangement of Equ. (10). By using SLS, the oil droplet size and shape can be determined independently of D, and the momentum transfer at the interface can then be determined using Equ (15). The combination of DLS and SLS experiments also has the benefit of using the same sample in both experiments, which provides several internal checks for self-consistency between the two analyses. In addition to determining α, SLS confirms the droplets' spherical shape and is used to determine κa which is an important parameter in theoretical predictions of electrophoretic mobility as a function of ζ-potential.

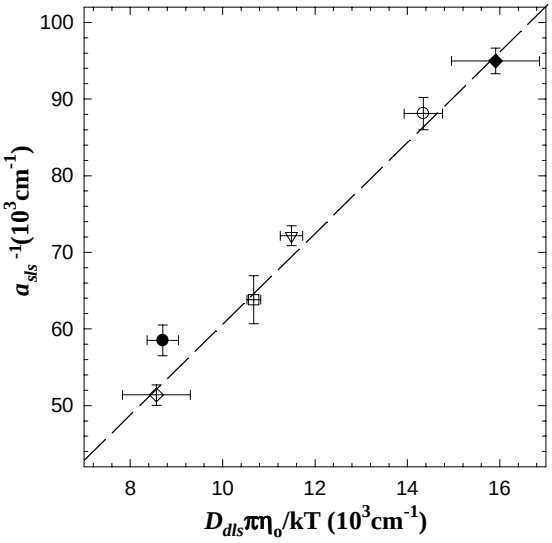

Figure 4: Inverse of the radius obtained from SLS measurements, (a_{sls}^{-1}), as a function of the quantity $D\pi\mu/kT$, with the diffusion coefficient, D, obtained from DLS measurements. IDC latex (♦), synthesized latex (•), decane droplets in SDS concentrations (O) 5 mM, (∇) 1 mM, ( ) 0.5 mM, (◊) 0.1 mM. Fitted line (--) for the SDS/decane droplets gives α=6.12.

The results of the SLS and DLS experiments are summarized in Fig. 4. The inverse of the radius, a_{sls}^{-1} is shown as a function of $D_{dls}\pi\eta/kT$ for solid particles and droplets with an average $\alpha/(\pi\eta a)$=6.12 from the regressed slope. Polystyrene (PS) solid particles at either end of the size range of the SDS/decane droplets have been used to confirm the validity of this technique. The SLS and DLS data for both the SDS/decane droplets and PS particles are consistent with the droplets behaving as non-deformable, solid, monodisperse spheres with no internal flow, since they give $\alpha/(\pi\eta a)$=6 within experimental error. Although some degree of polydispersity in the droplet size is certainly present, the quality of the curve-fits for SLS and DLS data, which assume monodispersity are more than adequate for quantitative analysis of the droplet α.

The oil droplet radii are also observed to decrease with increasing SDS concentration which is consistent with a reduction in the droplet interfacial tension, or Laplace pressure, however, the oil volume fraction was not controlled to allow for quantitative examination of this trend. Finally, droplet shape fluctuations were not evident within the DLS temporal or SLS spatial resolutions, and are probably unimportant for interpreting droplet electrophoresis.

Interpretation of ζ-potentials from Interfacial Tension Data (SDS Surface Excess)

From Table 2, 3 ζ-potential options all have $\alpha/(\pi\eta a)$=6 and therefore remain reasonable choices. In order to make further progress in interpreting μ, it is relevant to consider SDS surface excess data obtained from

SDS/decane interfacial tension measurements. Although the light scattering data provide information concerning droplet hydrodynamics relevant to electrophoresis, the SDS surface excess can be used to understand the possible ζ-potentials in terms of interfacial surfactant counter-ion binding.

The Gouy-Chapman model was used to relate surface potential, and surface charge density, σ, of a charged interface[25]. Interfacial tension data were measured using the pendant droplet technique at 298K. The surface excess of surfactant with respect to the bulk SDS concentration was calculated from the Gibbs equation[26, 27]. The fraction of interfacial SDS without bound counter-ion is interpreted as the ratio of the charge corresponding to the ζ-potential to the charge for completely ionized interfacial SDS. This fraction is defined by,

$$f = \frac{\sigma_\zeta}{\sigma_\Gamma} = -\frac{2kT\varepsilon_o\varepsilon_w\kappa}{\Gamma e^2}\cdot sinh\left[\frac{e\zeta}{2kT}\right] \tag{16}$$

where f indicates the fraction ionized, σ_ζ is the surface charge corresponding to the surface potential of a charged interface, σ_Γ is the surface charge density corresponding to complete surfactant ionization which can be determined by expressing the surface excess as a number area density and multiplying by the unit charge. The other symbols have their usual meaning.

Values of f are plotted in Fig. 5 as a function of bulk SDS concentration for the data in Table 2, which are the remaining ζ-potential after consideration of the light scattering measurements of α. Easily dismissible are the ζ-potentials that correspond to f>1 which are unphysical. For the 0.01mM SDS case, this leaves one choice, the low ζ-potential rigid droplet solution. For the 0.1mM case, ζ=-125 mV with f =0.2 appears to be the best option. The next higher ζ-potential with f=0.61 is very high compared to literature values for previous SDS-oil-water interface studies[28, 29]. The 0.01 and 0.1 mM SDS cases have less interfacial surfactant, but give the low ζ-potential rigid droplet solution suggesting the same solution for the 1 mM SDS case. A surface potential independent of the adsorbed amount is reasonable since counter ion binding can adjust to compensate for lateral interactions and preserve the potential or charge.

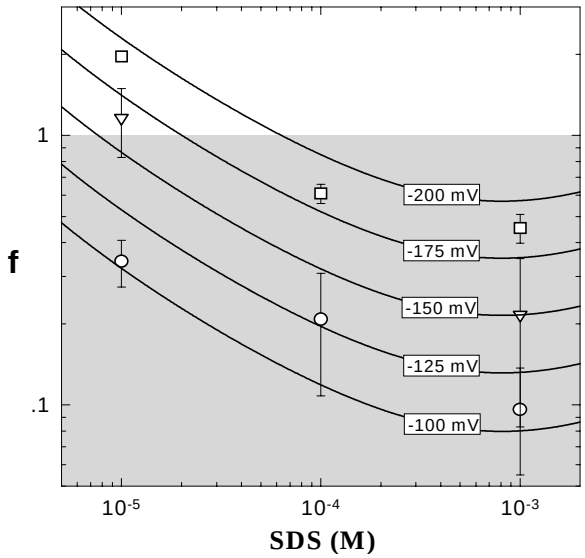

Figure 5: Fraction ionization from Equ. (16). Values calculated by comparing of surface charge density inferred from ζ-potentials in Table 2 and surface charge density inferred from surface excess assuming complete ionization. For each SDS concentration, three ζ-potentials possible from electrophoretic mobility data (after considering light scattering data): Solid 1(O), Solid 2 (∇), and Liquid 2 ( ). For reference in Fig. 5, curves showing f as a function of constant ζ-potential are shown for ζ= -100, -125, -150, -175, and -200 mV.

With the surface tension and light scattering data, it is possible chose a single ζ-potential between -100 mV to -125 mV for each SDS concentration. These ζ-potentials can now be used comparing the theory to experimental data and to allow a further understanding of the forces occurring at 'soft' interfaces.

Comparison of Experimental Data and Theoretical Model

An example of the theory and experimental data for 10^{-3} M SDS / 10^{-3} M $NaNO_3$ is shown in Fig. 6. With the knowledge of the oil droplet surface potential, the experimental data has been shown to be successfully modelled. The minimum separation between the oil droplet and the colloidal probe occurs at 92 Angstroms.

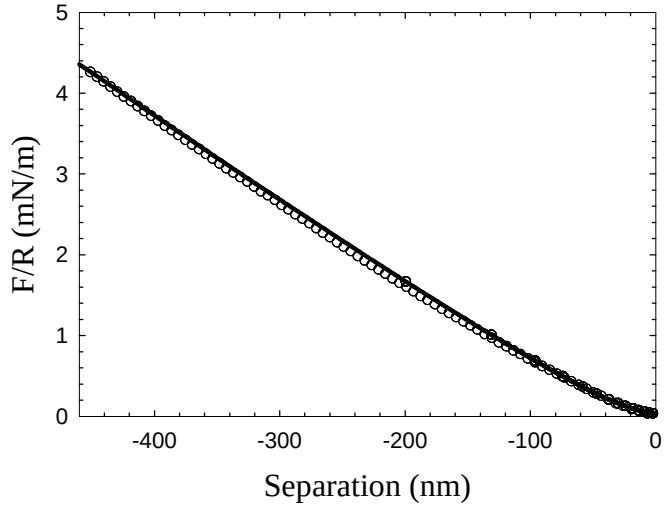

Figure 6: Force/Radius vs. Separation for 10^{-3} M SDS / 10^{-3} M $NaNO_3$. Experimental Data (O), Model (-). Parameters used in model are experimentally determined and are as follows: Interfacial tension, γ = 28 dyne/cm, Contact Angle, $\theta_c = 78^o$, Probe radius, a =2.16μm, Drop Radius, R_o = 50μm, Potential of Silica = -50 mV, Surface Potential of *n*-decane = -100 mV.

CONCLUDING REMARKS

The forces of interaction between a colloidal probe and a liquid-liquid interface have been measured in different solutions. The apparent interplay between interfacial deformation and double layer interactions in these experiments has important implications in understanding both emulsion stability and wetting phenomena. It demonstrates that control of these characteristics may be achieved through a balance of interfacial electrostatics and tensions.

To understand and model the interactions of a solid particle approaching a liquid interface, an independent determination of the surface potential on the liquid interface was required. For the system dealt with here, the SDS/decane droplets all have ζ-potentials between -100 mV to -125 mV with no obvious dependence on bulk SDS concentrations between 0.01-1 mM. The combination of light scattering and surface tension experiments permit the unambiguous conversion from electrophoretic mobility, μ, to ζ-potential. The surfactant coated oil droplets were also shown to behave like solid particles in terms of their hydrodynamic mobility for all SDS concentrations studied here. In addition, we demonstrated that when using SDS at concentrations below the CMC in the presence of decane, stable and reproducible monodisperse oil droplets can be produced with sonication.

The theoretical model that calculates the force between a rigid spherical probe particle and a liquid interface has been shown to successfully model the experimental data obtained from AFM measurements.

ACKNOWLEDGEMENTS

This work was supported by the Australian Research Council and the Particulate Fluids Processing Centre at the University of Melbourne. SAN is a recipient of the Howard K. Worner Scholarship funded by BHP and Riotinto and an Australian Postgraduate Award. We are grateful to Dr David Dunstan of the Department of Chemical Engineering/CRC for Bioproducts for providing use of the Malvern 4700 light scattering apparatus.

REFERENCES

1. Israelachvili, J.N., (1991), *Intermolecular and Surface Forces*. 2nd ed. London: Academic Press.
2. Ivanov, I.B. and Dimitrov, D.S., in *Thin Liquid Films*, I.B. Ivanov, Editor. 1988, Dekker: New York. Chapter 8.
3. Ivanov, I.B. (1980) 'Dynamic Behaviour of Liquid Films', *Pure Appl. Chem.*, **52**, 1241.

4. Ivanov, I.B., Dimitrov, D.S., Somasundaran, P., and Jain, R.K. (1985) 'Thinning of Films with Deformable Surfaces: Diffusion-Controlled Surfactant Transfer', *Chem. Eng. Sci.*, **44**, 137.
5. Traykov, T.T. and Ivanov, I.B. (1977) 'Hydrodynamics of thin liquid films. Effect of surfactants on the velocity of thinning of emulsion films.', *Int. J. Multiphase Flow*, **3(5)**, 471.
6. Zhang, X. and Davis, R.H. (1991) 'The Rate of Collisions due to Brownian or Gravitational Motion of Small Drops', *Journal of Fluid Mechanics*, **230**, 479.
7. Yiantsios, S.G. and Davis, R.H. (1991) 'Close Approach and Deformation of Two Viscous Drops due to Gravity and van der Waals Forces', *J. Colloid Interface Sci.*, **144**, 421.
8. Kelsall, G.H., Tang, S., Yurdakul, S., and Smith, A.L. (1996) 'Electrophoretic behaviour of bubbles in aqueous electrolytes', *J. Chem. Soc., Faraday Trans.*, **92(20)**, 3887-3893.
9. Chan, D.Y.C., Dagastine, R.R., and White , L.R. (2001) 'Forces between a Rigid Probe Particle and a Liquid Interface, I. The Repulsive Case', *J. Colloid Interface Sci.*, **236(1)**, 141.
10. Hunter, R.J., (1981), *Zeta Potential in Colloid Science*. London: Academic Press Inc.
11. Baygents, J.C. and Saville, D.A. (1991) 'Electrophoresis of Drops and Bubbles', *J. Chem. Soc., Faraday Trans.*, **87(12)**, 1883-1898.
12. Hartley, P.G., Grieser, F., Mulvaney, P., and Stevens, G.W. (1999) 'Surface forces and deformation at the oil-water interface probed using AFM force measurement', *Langmuir*, **15(21)**, 7282.
13. Chan, D.Y.C., Pashley, R.M., and White, L.R. (1980) 'A Simple Algorithm for the Calculation of the Electrostatic Repulsion between Charged Identical Charged Surfaces in Electrolyte', *J. Colloid interface Sci.*, **77(1)**, 283.
14. von Smoluchowski, M. (1903) 'Contribution à la théorie de l'endosmose électrique et de quelques phenomènes corrélatifs.', *Bulletin international de l'Académie des Sciences de Cracovie*, **8**, 182.
15. Levich, V.G., (1962), *Physicochemical Hydrodynamics*. N. J.: Prentice-Hall.
16. Ohshima, H., Healy, T.W., and White, L.R. (1984) 'Electrokinetic Phenomena in a Dilute Suspension of Charged Mercury Drops', *J. Chem. Soc., Faraday Trans. 2*, **80**, 1643.
17. Levine, S. and O'Brien, R.N. (1973) 'A Theory of Electrophoresis of Charged Mercury Drops in Aqueous Electrolyte Solution', *J. Colloid Interface Sci.*, **43(3)**, 616.
18. Baygents, J.C. and Saville, D.A. (1991) 'Electrophoresis of Small Particles and Fluid Globules in Weak Electrolytes', *J. Colloid Interface Sci.*, **146(1)**, 9.
19. Ohshima, H. (1997) 'A Simple Expression For the Electrophoretic Mobility of Charged Mercury Drops', *J. Colloid Interface Sci.*, **189(2)**, 376.
20. Barchini, R. and Saville, D.A. (1996) 'Electrokinetic Properties of Surfactant-Stabilised Oil Droplets', *Langmuir*, **12**, 1442-1445.
21. Dunstan, D.E. and Saville, D.A. (1992) 'Electrophoretic Mobility of Colloidal Alkane Particles in Electrolyte Solutions', *J. Chem. Soc., Faraday Trans.*, **88(14)**, 2031.
22. Dunstan, D.E. (1994) 'Temperature Dependence of the Electrokinetic Properties of Two Disparate Surfaces', *J. Colloid Interface Sci.*, **166(2)**, 472.
23. O'Brien, R. and White, L.R. (1978) 'Electrophoretic Mobility of a Spherical Colloidal Particle', *J Chem Soc., Faraday Trans. 2*, **74**, 1607.
24. Happel, J. and Brenner, H., (1965), *Low Reynolds number hydrodynamics*. N. J.: Prentice-Hall, Inc.
25. Russel, W.B., Saville, D.A., and Schowalter, W.R., (1989), *Colloidal Dispersions*. Cambridge, U.K.: Cambridge University Press.
26. Tajima, K. (1971) 'Radiotracer Studies on Adsorption of Surface Active Substance at Aqueous Surface. III. The Effects of Salt on the Adsorption of Sodium Dodecylsulfate', *Bull. Chem. Soc., Jpn*, **44(7)**, 1767.
27. Hall, D.G., Pethica, B.A., and Shinoda, K. (1975) 'The Interpretation of Surface Tension Data for Solutions of Ionic Surfactants in the Presence of Electrolyte', *Bull. Chem. Soc., Jpn*, **48(1)**, 324.
28. Haydon, D.A. and Taylor, F.H. (1960) 'On Adsorption at the Oil/Water Interface and the Calculation of Electrical Potentials in the Aqueous Surface Phase I. Neutral Molecules and a Simplified Treatment for Ions', *Philos. Trans. R. Soc.*, **252**, 225.
29. Kalinin, V.V. and Radke, C.J. (1996) 'An Ion-Binding Model For Ionic Surfactant Adsorption At Aqueous-Fluid Interfaces', *Colloids Surf., A*, **114**, 337.